

Article

Effect of Cold Rolling Prior to Annealing on the Grain Size-Energy Losses Relationship in a Low Carbon Grain Non-Oriented Semi-Processed Electrical Steel

Nancy Margarita López-Granados ^{1,*}, Emmanuel José Gutiérrez-Castañeda ²
and Armando Salinas-Rodríguez ³

¹ TecNM/I.T. Morelia, Tecnológico 1500 Av., Morelia 58120, Mexico

² Institute of Metallurgy, Materials Engineering, Universidad Autónoma de San Luis Potosí, San Luis Potosí 78210, Mexico; emmanuel.gutierrez@uaslp.mx

³ Centro de Investigación y de Estudios Avanzados del Instituto Politécnico Nacional, Saltillo 25000, Mexico; armando.salinas@cinvestav.edu.mx

* Correspondence: nancy.lg@morelia.tecnm.mx

Abstract: In this work, the effect of cold deformation prior to annealing treatment on the microstructure and magnetic hysteresis energy losses in a low carbon grain non-oriented semi-processed electrical steel with 0.60 mm thickness was investigated. The samples were subjected to different percentages of deformation, in a range of 5–20% reduction and annealed at temperatures between 650 and 950 °C for 60 min, these were characterized by Optical Microscopy. Meanwhile the energy losses were calculated from the magnetic hysteresis loops using a Vibrating Sample Magnetometer. The experimental results showed that cold deformation increases energy losses by 50% when the steel is deformed 20%, due to microstructural defects that are introduced to the material during deformation. The presence of the microstructural defects was verified through measurements of Full Width at Half Maximum by means of X-ray diffraction. On the other hand, it was observed that annealing at temperatures below A_{c1} causes only small changes in the microstructure of the steel, however, it promotes the recovery of magnetic properties by 50% with respect to the deformed material. In contrast, when the material is annealed between A_{c1} and A_{c3} ($\alpha + \gamma$) magnetic properties are recovered ~33% with respect to the initial state and, at values higher than 65% compared to the state of greatest deformation (20%), as a result of both microstructural modification and the evolution of the grain size experienced by the material.

Keywords: electrical steel; energy losses; grain size; microstructure; lamination; annealing; magnetometer



Citation: López-Granados, N.M.; Gutiérrez-Castañeda, E.J.; Salinas-Rodríguez, A. Effect of Cold Rolling Prior to Annealing on the Grain Size-Energy Losses Relationship in a Low Carbon Grain Non-Oriented Semi-Processed Electrical Steel. *Metals* **2022**, *12*, 1211. <https://doi.org/10.3390/met12071211>

Academic Editor: Francesca Borgioli

Received: 1 June 2022

Accepted: 7 July 2022

Published: 17 July 2022

Publisher's Note: MDPI stays neutral with regard to jurisdictional claims in published maps and institutional affiliations.



Copyright: © 2022 by the authors. Licensee MDPI, Basel, Switzerland. This article is an open access article distributed under the terms and conditions of the Creative Commons Attribution (CC BY) license (<https://creativecommons.org/licenses/by/4.0/>).

1. Introduction

The generation, transmission and transformation of energy are the pillars of modern industry. In these processes devices such as transformers, generators and electric motors are the main protagonists. The cores of these devices are manufactured using electrical steels, which are soft magnetic materials and rank first in importance among magnetic materials worldwide in terms of tonnage and value produced in the market. Approximately, 50% of the worldwide produced electrical energy is used in motors, and the awareness of the need to save energy has generated interest in the development of high-performance electrical steels [1]. There are two types of electrical steels: grain oriented -GO- and grain non-oriented (GNO). The appropriate microstructural characteristics that lead to optimal magnetic properties are obtained through steel processing. Losses of magnetic properties in electrical steels are sensitive to both chemical composition (Si + Al) and structure, and are highly dependent on a number of metallurgical factors, such as material cleanliness, crystallographic texture, grain size and shape, the stress-strain state, and the existence of anisotropic distributions of some microstructural elements such as secondary phases,

inclusions, etc., [2,3]. Manufacture of final forms from electrical steel sheets includes additional deformation processes, all these forming operations have a determining effect on energy losses and magnetic permeability due to the effect they cause on grain size and texture. Therefore, it is very important to assess the extent of the deterioration of the magnetic properties when the steel is plastically deformed [4,5]. Several investigations have been conducted on these topics. Hou [6] found that the magnetic losses are directly proportional to the dislocation density generated by rolling. Shiozaki et al. [7] carried out a study to relate magnetic hysteresis losses, grain diameter and silicon content by means of an equation, under different magnetic field conditions, reporting that hysteresis losses are proportional to grain size, while eddy current losses are inversely proportional to grain diameter. Jiles et al. [8] pointed out that the energy loss to pinning is proportional to the density and average pinning energy of dislocation. Bailey and Hirsch [9] demonstrated that the flow stress is proportional to the square root of the dislocation density. Accordingly, dislocations exert a considerable effect on magnetic properties [10]. The generation and accumulation of dislocations in a disorderly manner produce entanglements that are fixation centers for the walls of the magnetic domains, therefore, they prevent their free movement, which generates an important effect on magnetic hysteresis. In contrast, other investigations asseverate [11–13], that as the grain size increases, the hysteresis losses decrease while the eddy current losses increase, therefore, there is an optimal grain size that minimizes the total energy losses. These results suggest that when the material is treated at high temperatures, the residual stresses are decreased, in addition, the recrystallization and grain growth processes are activated depending on the imposed deformation degree [14,15], which indicates that, there is the possibility to produce electrical steel sheets with acceptable, even better, magnetic characteristics with short annealing times [16,17]. In general, GNO electrical steels are manufactured from continuous casting by hot rolling, cold rolling, continuous annealing or batch annealing and temper rolling [18]. Subsequently, they are subject to long periods of heat treatment at temperatures below A_{c1} to promote decarburization and grain growth. Recently, different investigations [19–21] have proposed alternative processing routes to improve the production processes for different grades of electrical steels. These include optimization of hot rolling, annealing prior to cold deformation or rolling in stages with intercritical annealing, obtaining a good relationship of mechanical-magnetic properties in electrical steels with Si + Al contents greater than 1%. Therefore, this investigation offers a methodology that allows evaluating the effect of cold deformation and annealing heat treatment on the microstructure and magnetic properties of a low carbon GNO semi-processed commercial electrical steels with low Si + Al content (~0.6%). The results obtained indicate that it is possible to obtain electrical steels with low magnetic losses and high permeability, when they are subjected to a cold deformation process prior to the annealing stage, at relatively low temperature, between A_{c1} and A_{c3} ($\alpha + \gamma$) and short times (1 h). The described, allow the recovery of magnetic properties in ~33% with respect to the initial state and higher than 65% when it has been deformed, taking advantage of those obtained by conventional batch annealing processing during 16 h at 750 °C. The proposed processing route converts the used material in this investigation into very attractive product which is favorable to both energy and socioeconomic aspects.

2. Materials and Methods

A commercial semi-processed grain non-oriented electrical steel sheet with a thickness of 0.60 mm was used as research material. Table 1 shows the chemical composition (wt%) determined by optical emission spectroscopy based on the ASTM E-403 standard. Critical transformation temperatures (A_{c1} and A_{c3}) were calculated by dilatometric analysis, the values obtained were 722 °C and 912 °C, respectively. In this case, 20 samples of 15 cm wide by 30 cm long were cut from the tail-end of the GNO electrical steel coil. Subsequently, they were cold deformed at 5, 10 and 20% in stages (0.01 mm thickness reduction per pass) in the original rolling direction, in a HILLE Helicon MK4 Series 2 rolling mill, at a roll rotation speed of 18 rpm and with the use of lubricant to reduce friction. 5 samples

were cold rolled for each of the rolling conditions. The final thicknesses after reduction were: 0.57, 0.54 and 0.48 mm, respectively. The annealing heat treatments of the initial state and deformed samples were carried out in a muffle furnace in air atmosphere at temperatures of 650 °C, 750 °C, 850 °C and 950 °C for 60 min at an average heating rate of 10 °C/min and subsequent air cooling. In order to have a strict control of the temperature during the thermal cycles, samples were instrumented with thermocouples (K-type). The reading of the thermocouples was recorded by means of a FLUKE model 2680 data acquisition system. Samples for microscopic examination were prepared by conventional metallographic techniques and etched with 3% Nital during 7 s to reveal the material microstructure. Microstructural characterization of the deformed and annealed samples was carried out using an Olympus Vanox AHMT3 model (Tokyo, Japan) metallographic microscope. The images were processed in an image analyzer with the Image Pro-Plus program (version 7.0), while the average grain size for each of the experimental conditions was calculated by the linear intercept method based on the ASTM E-112 standard [22]. To obtain a representative result, 10 fields were measured and, 10 lines were used for each sample. The samples analyzed by X-ray diffraction (Bruker, Billerica, MA, USA, D8 Advance), were cut in dimensions of 1 cm long × 1 cm wide, both for the deformed steel (5–20%) as well as for sample subject to the highest percentage of deformation (20%) and annealed at different temperatures (650–950 °C). The normal planes of both deformed and annealed samples were grinded and polished to achieve a mirror-like surface. Analysis was performed using CuK α monochromatic radiation ($\lambda = 0.15418$ nm), 35 kV, 25 mA, step 0.02°, scan rate 2°/min and 2 θ range 0–160°. The full width half maximum (FWHM), defined as the width of the distribution at a level that is just half the maximum ordinate of the peak, was calculated with the software DIFFRAC.EVA 5.2 from XRD data for the diffraction peaks (100), (200), (211), (220) and (222). FWHM was then associated with the dislocation density in the analyzed samples. Finally, magnetic properties were measured on a Lake Shore Series 7300 VSM System vibrating sample magnetometer (Lake Shore Cryotronics, Inc., Westerville, OH, USA 1993) at 50 Hz. The electrical steel samples were magnetized until reaching saturation magnetization at 2.1T [23,24]. 10 samples of 1 mm wide × 3 mm long were cut, with an approximate weight between 25 and 30 mg. 10 samples were analyzed for each experimental condition. Through the Lake Shore VSM version 3.0 program, the magnetic hysteresis cycles were obtained, which allowed calculating the coercivity, remanence, and energy losses.

Table 1. Chemical composition of steel (wt%).

Element	Si	C	Mn	Al	Cr	P	Mo	Ti	Nb	S	Fe
%	0.383	0.03	0.594	0.217	0.053	0.043	0.018	0.003	0.0002	<0.0005	98.56

3. Results and Discussion

3.1. Effect of Plastic Deformation on Microstructure and Magnetic Properties

Microstructures of the samples in the initial state (without deformation) and deformed at 5, 10 and 20% are shown in Figure 1. As can be seen, there are no significant changes in the morphology of the ferrite grains associated with the applied plastic deformation. The microstructure of the deformed samples Figure 1b–d have morphological characteristics very similar to the initial state as show in Figure 1a. In Figure 1c,d some deformation lines can be observed, as well as small elongated grains located in the vicinity of the bands, as a result of higher percentage of lamination imposed on the material. In general, all the samples exhibit quasi-equiaxial ferrite grains, with a heterogeneous grain size of approximately 25 μ m.

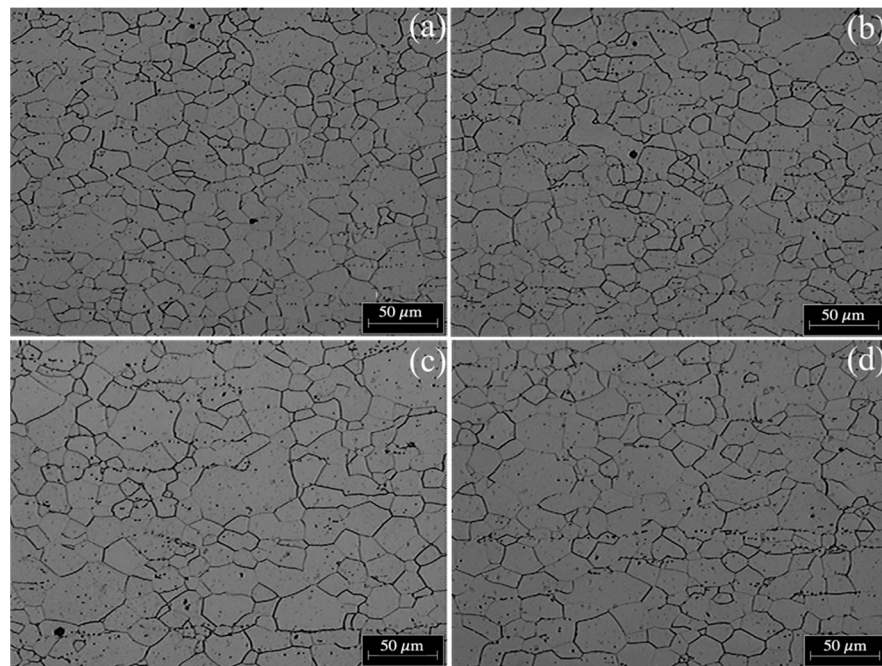


Figure 1. Microstructures of deformed semi-processed grain non-oriented electrical steel (a) 0%, (b) 5%, (c) 10% and (d) 20%.

ASTM A683 standard [25] establishes values of energy losses in the cores made of semi-processed grain non-oriented electrical steel from the Si + Al contents measured in the Epstein frame at 1.5T, at 50Hz and 60Hz. For contents close to 1% Si + Al, the standard indicates an energy loss value of ~6.1 W/kg. Figure 2 shows the effect of deformation on the magnetic properties of the studied steel. The properties were calculated from the magnetic hysteresis curves obtained in the VSM. It can be seen in Figure 2a that the coercivity increases to values close to 75% with respect to the initial state as the deformation increases. The deformation effect on the coercive force is well known, since it increases the area of the hysteresis loop, which leads to a decrease in permeability. In contrast, in Figure 2b it can be seen that the remanence decreases as a consequence of the deformation imposed on the material. However, such behavior is not desirable since it is one of the characteristic required in steel. Figure 2c shows the energy losses for the steel without deformation and with different percentages of deformation (5–20%). In the case of steel in the undeformed state, the losses correspond to 3.4 W/kg according to the ASTM A683 standard. The value obtained is related to the chemical composition of the material, since the Si + Al content for the steel used in this investigation is approximately 0.59%, which is 40% lower than the minimum value reported in the standard. Meanwhile, in Figure 2c it can be seen that the graph experimentally obtained exhibits an almost linear behavior, in such a way that, as the deformation increases, the energy losses increase proportionally. The most important change is obtained when the steel is deformed above 10%, since the sample with the highest percentage of deformation (20%) exhibits a 50% increase in magnetic hysteresis losses compared to the undeformed state, reaching values higher than 6.7 W/kg. The behavior observed in the properties is due to the introduction of defects in the microstructure, mainly to the dislocations accumulation in a disorderly manner [26]. The last agrees with those pointed out by some researches [9,10], where they establish that the main mechanism to explain the deterioration of the magnetic properties is related to the interaction between the magnetic domains wall and the dislocation density associated with deformation.

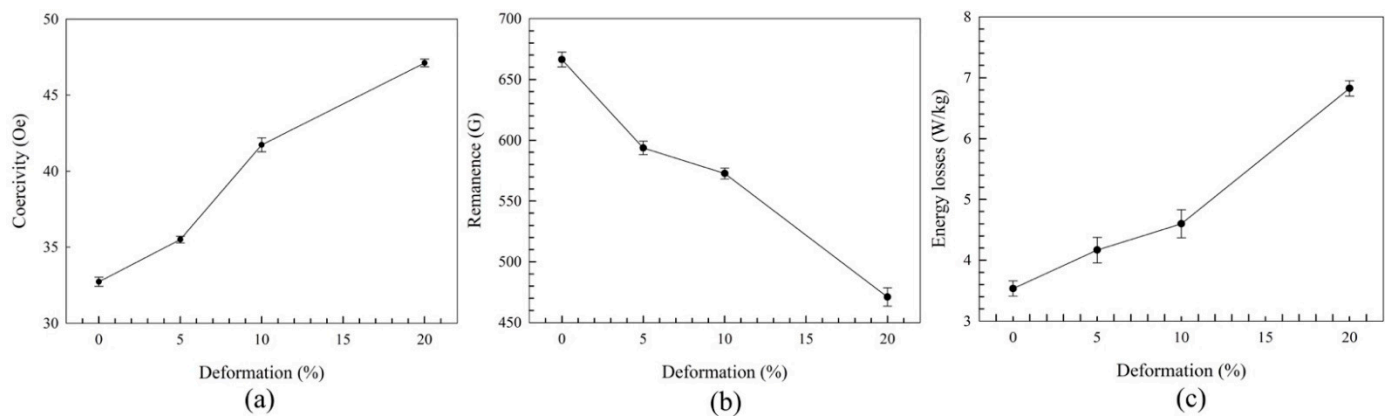


Figure 2. Effect of deformation on the magnetic properties of steel: (a) coercive field, (b) remanence, (c) energy losses.

When a material undergoes non-uniform deformation, as in the case of a grain embedded in a polycrystal, depending on the orientation of neighboring grains, the crystal planes can be compressed or stretched. Therefore, the X-ray diffraction peaks of the deformed material show a decrease in maximum intensity and an increase in width at half the maximum intensity—FWHM—[27]. Figure 3 shows the effect of plastic deformation on the FWHM for the most important diffraction peaks obtained by X-ray diffraction of the steel studied. As can be seen, the FWHM significantly increases as the strain, however, the changes are more significant in the case of peaks (220) and (222), even with low strain values (between 5 and 10%). The increase in FWHM is mainly associated with dislocation density and non-uniform strain across the sheet microstructure. As the strain increases, the number of defects introduced to the material increases considerably. These defects (dislocations) are not found in the structure of the material in an orderly manner, and due to this disorder, when the material is exposed to a magnetic field, high coercive fields are required to force the magnetic dipoles to align in the direction that the magnetic field is being applied (see Figure 2a), since the crystalline defects act as barriers obstructing the rotation of the magnetic dipoles, which increases the area of the hysteresis loop and, consequently, increases the energy losses as can be seen in Figure 2c [3,5–9].

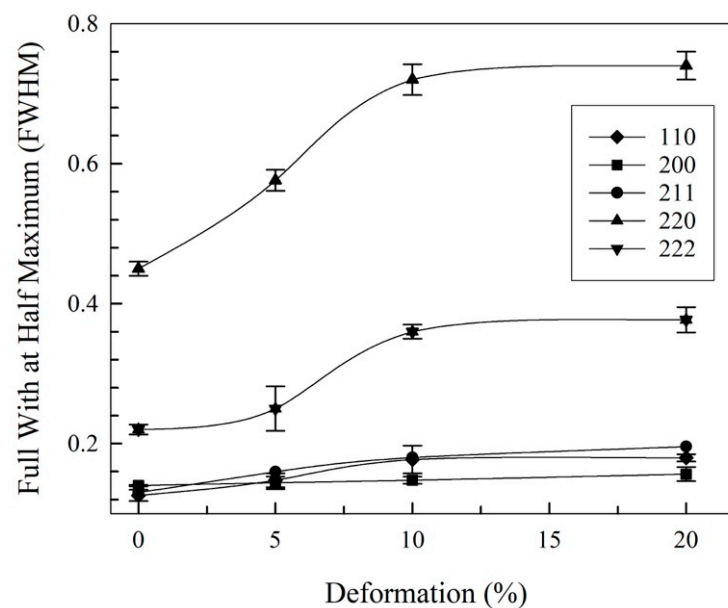


Figure 3. Effect of plastic deformation on the FWHM for different diffraction peaks.

3.2. Effect of Annealing Temperature on the Microstructure

Figure 4 shows the effect of annealing temperature on the microstructure of the deformed samples. As can be seen, annealing causes important changes in morphology and ferrite grain sizes as the treatment temperature increases. Figure 4a shows the results corresponding to the samples treated at 650 °C ($T < A_{c1}$); as can be seen, the microstructural characteristics between the original and deformed samples (5–20%) are very similar. In general, the microstructure is composed of ferrite grains with equiaxed morphology and a non-uniform size of ~28 µm. These results suggest that annealing in the ferrite phase field ($\alpha - Fe$, $T < 722$ °C), only causes some effects associated with the rearrangement of dislocations or the released of residual stresses. In contrast, the microstructural modification of the annealed samples in the intercritical region ($\alpha + \gamma$) is remarkable. Figure 4b shows the micrographs of the steel annealed at 750 °C. As can be seen, the microstructures of samples with deformations equal or lower than 10% are characterized by the presence of a non-uniform microstructure constituted by a mixture of large ferrite grains located on the edge of the sheet, and smaller grains in the center. For the same temperature, the microstructure of samples with 20% of deformation shows large ferrite grains with average grain size of about 130 µm, which suggests that the small grains have completely been consumed. A similar type of growth is observed when temperature is increased up to 850 °C, Figure 4c. A mixture of large and small ferrite grains is obtained for deformation levels equal or lower than 10%, but for a higher deformation degree (20%), only large ferrite grains with average grain size of about 170 µm are observed. The amount of small grains observed in samples annealed at 750 °C and 850 °C, tend to decrease with the increase in the deformation level. Furthermore, for a given deformation condition, the size of both small and large grains, increases with the increase in temperature from 750 °C to 850 °C. These results suggest that the kinetic of the abnormal growth occurs faster with the increase in the strain level and temperature. Similar results were reported for a steel containing 0.07 wt% C and Si + Al = 0.78 wt%, after tensile deformations of 8%, 12% and 25% and subsequent annealing at 700 °C and 800 °C. It was observed that, annealing at these temperatures, in samples with 8% and 12% of deformation, resulted in microstructures consisting of a mixture of large and small ferrite grains. In contrast, annealing in samples with previous deformation of 25%, resulted in microstructures consisting mainly on larger and equiaxed ferrite grains [28]. They found that abnormal growth in samples with 12% of deformation was faster than in samples with 8% of deformation, and the effect was more significant at 800 °C, which is a similar behavior than the one observed in the present work. The abnormal growth was explained in terms of the so-called strain induced boundary migration (SIBM) mechanism, which commonly occurs in materials with low deformation [28]. Growing of grains by SIBM initiate in high-strain grains and progresses until a new low-strain grain is formed and separated from the original; growing is driven by minimization of stored energy leading to a lower strain condition. Growth is followed by coalescence of grains resulting in larger grains as observed in Figure 4b,c. Figure 4d shows the microstructures of the samples thermally treated at $T > A_{c3}$ (912 °C). The microstructure of the undeformed sample consists mainly of large ferrite grains (average size > 100 µm), which suggest that the abnormal growth is favored by the increase in temperature due to a higher driving force for grain boundary motion, compare the microstructures of samples without deformation in Figure 4c,d. A different behavior is observed in samples with deformations of 5%, 10% and 20%, in this case, the grain size is significantly smaller than the one observed either in the undeformed condition or in samples annealed at 750 °C and 850 °C. The grain size decreases with the increase in the deformation level. In addition, it is important to notice that the grain size of samples annealed for 60 min at 950 °C ($T > A_{c3}$) is very similar than the one observed in samples annealed at 650 °C ($T < A_{c1}$), even when the driving force for grain boundary motion is higher ($\Delta T = 300$ °C). During heating of steel at temperatures above A_{c1} and below A_{c3} , austenite nucleates at ferrite grain boundaries and at carbides interfaces. Growth of austenite mainly occur during holding due to the more time available for boundary motion [29,30]. It appears then that the effect of deformation relies on the

increase in the number of nucleation sites. The higher the deformation, the higher the number of nucleation sites and the smaller the austenite grain, which on final cooling leads to a smaller ferrite grain. This could explain the reduction of grain size with the increase in the deformation level in samples annealed at 950 °C, Figure 4d. Some authors reported the simultaneous oxidation and decarburization process of an electrical steel containing 0.05 wt%C and Si + Al = 0.78 wt% during annealing conducted after hot-rolling [30]. The critical transformation temperatures reported for the steel used in such work were, $Ac_1 = 763$ °C and $Ac_3 = 946$ °C, which are about 41 °C and 34 °C higher than the critical temperatures of the steel used in the present work. Annealing was conducted in still air for 150 min at 700 °C, 750 °C, 800 °C, 850 °C, 950 °C and 1050 °C. It was found that annealing at temperatures below the Ac_1 (700 °C), causes only a marginal effect on the grain size. However, annealing in the intercritical region (800 °C, 850 °C), resulted in abnormal large ferrite grains with columnar structure, which grow from the surface towards the mid-plane of the steel thickness. They conclude that columnar grains are only formed if the decarburization annealing is performed in the two-phase field region and a sharp interface exists between the decarburized ferrite and two-phase area [30]. The quasi-equiaxial structure obtained in the present work at 750° and 850 °C, which differs from the columnar structure reported by these authors at 850 °C, can be related to variations in the critical temperatures. For the same temperature, the proportions of austenite and ferrite during the thermal treatment should be different, and this can affect the steel decarburization kinetics and grains morphology. These authors also found that, annealing at temperatures above the Ac_3 (950 °C, 1050 °C) led to small and equiaxed ferrite grains, which were significantly smaller than those observed after annealing in the two-phase field region (800 °C, 850 °C). Annealing at $T \geq 950$ °C caused a reduction in the variation of decarburization, which was attributed to the combination of large oxide thickness and the absence of defects (pores or cracks) in the oxide structure. These results are similar to the ones observed in the present work in deformed samples, the increase in the annealing temperature from 850 °C to 950 °C leads to a significant reduction in grain size, compare Figure 4c,d. Some authors conducted an EBSD investigation on the abnormal columnar grain growth in non-oriented electrical steels [31]. They varied the deformation level (0%, 5%, 15%, 25%) applied to hot-rolled electrical steel bands and observed that, the abnormal grain growth that took place after annealing at 850 °C in the undeformed material, was not observed when the steel was deformed 15% prior to annealing at 850 °C. It was concluded that, the increase in the deformation level caused a more uniform distribution of strain along the steel thickness resulting in equiaxed grains. In such work, annealed samples exhibited shorter grain sizes for higher plastic deformation levels, which was related to higher nucleation sites. This behavior is also similar to the one observed in the present work. Therefore, it appears then that, the reduction in grain size in deformed samples annealed at temperatures above Ac_3 , is related to both the increase in the nucleation sites due to deformation and the variation in the oxidation/decarburization process at high temperatures [30,31]. On the other hand, independently of grain structure, from the magnetic properties point of view, it is expected that the increase in grain size obtained during intercritical annealing leads to a reduction of energy losses and to an increase in permeability, since the increase in grain size reduces the numbers of barriers that prevent the movement of the magnetic domain walls.

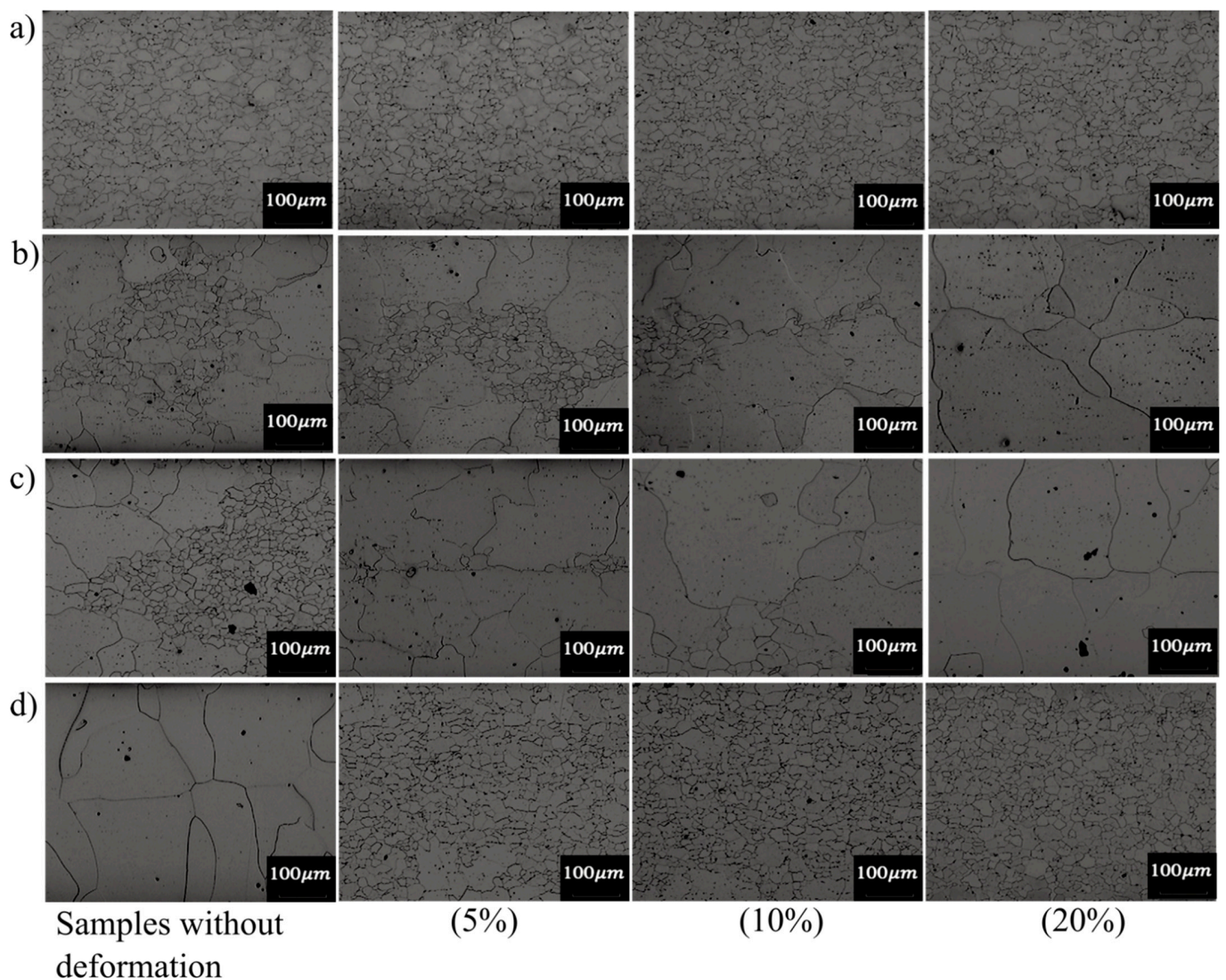


Figure 4. Microstructures of the semi-processed GNO electrical steel annealed at (a) 650 °C, (b) 750 °C, (c) 850 °C, (d) 950 °C, in initial condition (without deformation) and with prior deformation.

3.3. Magnetic Properties

Magnetic properties of the annealed samples for 60 min at different temperatures are shown in Figure 5. Annealing recovers all magnetic properties, only the remanence shows values very close to the sample in initial state. In Figure 5a it can be observed, the decrease in coercivity as the treatment temperature increases. Recovery is more important when annealing is carried out in the two-phase region ($\alpha + \gamma$). On the other hand, samples annealed at $T > A_{c3}$, show an opposite behavior, the coercive field increases as the deformation increases. Additionally, it can be seen that the sample without deformation annealed at 950 °C has a low coercivity values, even lower than the samples treated at $T < A_{c1}$ (650 °C). According to Figure 4, the described behavior is associated with the microstructure of the material, since the deformed samples (>10%) with treatment between 750 °C and 850 °C are composed of large ferrite grains. These same characteristics are shown in the sample without deformation annealed at 950 °C. Figure 5b shows the remanence values as a function of the deformation level and the annealing temperature. As can be seen, at temperatures between 750 °C and 850 °C, the highest remanence values are shown, which is favorable because remanence is a desired quality in electrical steel. However, treatment at high temperatures (950 °C) causes the opposite effect due to the decrease in grain size. Finally, in Figure 5c it can be seen that the most important recovery in

energy losses corresponds to the samples annealed at 850 °C, since even without previous deformation, the energy losses decrease from 3.4 W/kg to 3.1 W/kg, which relates to the changes observed in the microstructure by heat treatment. Similarly, it can be seen that by increasing the magnitude of the plastic deformation to 10% at the same annealing temperature (850 °C), the energy losses decrease by percentages greater than 50% with respect to the material in initial condition, due to that recover from 6.7 W/kg to 3.4 W/kg. However, the highest recovery in the magnetic properties was observed in samples with deformation of 20% and subsequent annealing at 850 °C, since it shows a decrease in energy losses greater than 65% (from 6.7 W/kg to 2.2 W/kg). On the other hand, it is important to highlight the unusual behavior shown in Figure 5c, where it is observed that the samples annealed at $T > A_{c3}$ shows higher loss values in the deformed samples. The undeformed steel annealed at 950 °C shows low energy losses, even lower than those of undeformed samples annealed at $T < A_{c1}$, although, the treatment is only effective for such treatment conditions. The behavior described above can be explained in terms of the microstructure showed in Figure 4, since the optimum grain size is obtained when the material is deformed above 10% and annealed in the intercritical range ($\alpha + \gamma$). However, higher temperatures promote a higher oxidation of steel as mentioned elsewhere [30], and thus affecting both steel decarburization and grain growth, and as a consequence, magnetic properties recovery is lower. The decrease in energy losses observed is related to different mechanisms; on the one hand, when steel is heat treated, internal stresses are released and rearrangement of the dislocation structure that were introduced during the deformation process occurs; on the other hand, the processes of recrystallization and grain growth are activated [7–12]. These phenomena are responsible for the recovery in the magnetic properties observed in the material, as a result of the decrease in the number of barriers that affect the magnetization process. Therefore, the magnetization process can be carried out at smaller magnetic fields compared to the deformed state, consequently reducing the area of the hysteresis loop [32–34]. Figure 6 shows the results of the X-ray diffraction analysis for the sample subject to the highest percentage of deformation (20%) and annealed at different temperatures. The diffraction peaks obtained via the FWHM show a considerable decrease compared to the deformed samples (see Figure 3). This behavior indicates that the internal stresses have been relieved and dislocations have been annihilated, therefore, it considerably improves the energy gain, which is in agreement with the results shown in Figure 5.

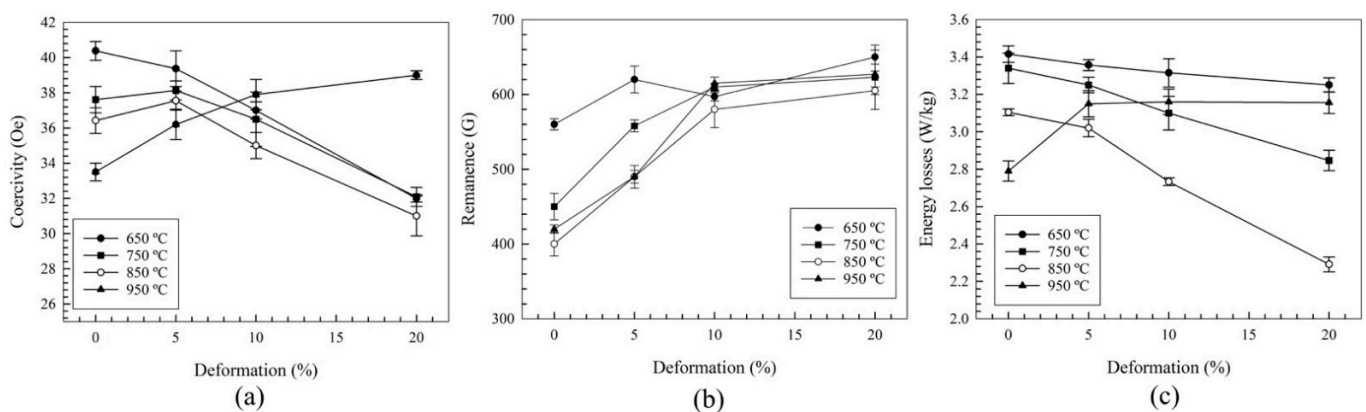


Figure 5. Effect of temperature on the recovery of energy losses in samples deformed at different percentages of reduction and annealed at different temperatures. (a) coercivity, (b) remanence, (c) energy losses.

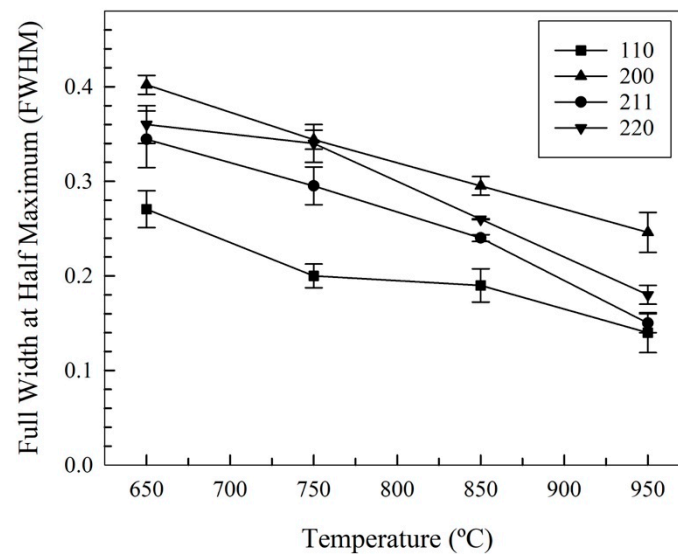


Figure 6. FWHM for different diffraction planes corresponding to the sample with 20% strain annealed for 60 min.

3.4. Magnetic Properties-Grain Size Relationship

Figure 7 shows the effect of annealing temperature on the grain size-energy loss relationship. In general, there is a decrease in energy losses as the annealing temperature increases, which is associated to grain growth. The sample without deformation (initial condition), shows grain sizes between ~ 28 and $100 \mu\text{m}$, when the steel is thermally at $T < A_{c1}$ and $T > A_{c3}$, respectively, which allows the energy loss values to be reduced by 3.2 and 2.9 W/kg, respectively. A similar behavior is observed in samples with 5% and 10% of deformation, however, this is only significant when the annealing is carried out at high temperature and high deformation, since the thermal treatment between $750 \text{ }^\circ\text{C}$ and $850 \text{ }^\circ\text{C}$ with $\sim 10\%$ deformations is not enough to complete the grain growth process. Therefore, average grain sizes of ~ 83.5 and $122 \mu\text{m}$, respectively, are reached; although, grain growth under such conditions is only partial, it allows to obtaining energy losses of less than 2.5 W/kg, which means a reduction of 27% with respect to the initial state and 63% in reference to the state with the greatest deformation. On the other hand, the best magnetic properties are obtained when the 20% deformed sample is subjected to annealing at $850 \text{ }^\circ\text{C}$, due to grain growth, reaching sizes $>170 \mu\text{m}$, which leads to a significant decrease of losses to 2.1 W/kg, and which represents a decrease of $\sim 70\%$. In contrast, the treatment at $T > A_{c3}$ of the deformed samples experiences a behavior opposite to that described above, due to the fact that the increase in energy losses is preferentially observed. In Figure 7, it can be seen that the losses are situated at 2.78 W/kg, which is slightly lower than that obtained in the treated samples $T < A_{c1}$ due to the decrease in grain size; therefore, the energy losses only are recovered to a limited extent. In the electrical steels case, the most important thing is to control the energy losses associated with the hysteresis cycle. To reduce losses, it is necessary to carry out the alignment and growth of the magnetic domains at low magnetic fields [35,36]. When grains grow, the amount of area and grain boundaries decrease, therefore, the number of barriers that limit the growth and free movement of the magnetic domains walls decrease considerably and, in this way, the magnetization process becomes energetically economical, so that the results described above reasonably support the findings obtained in the investigation.

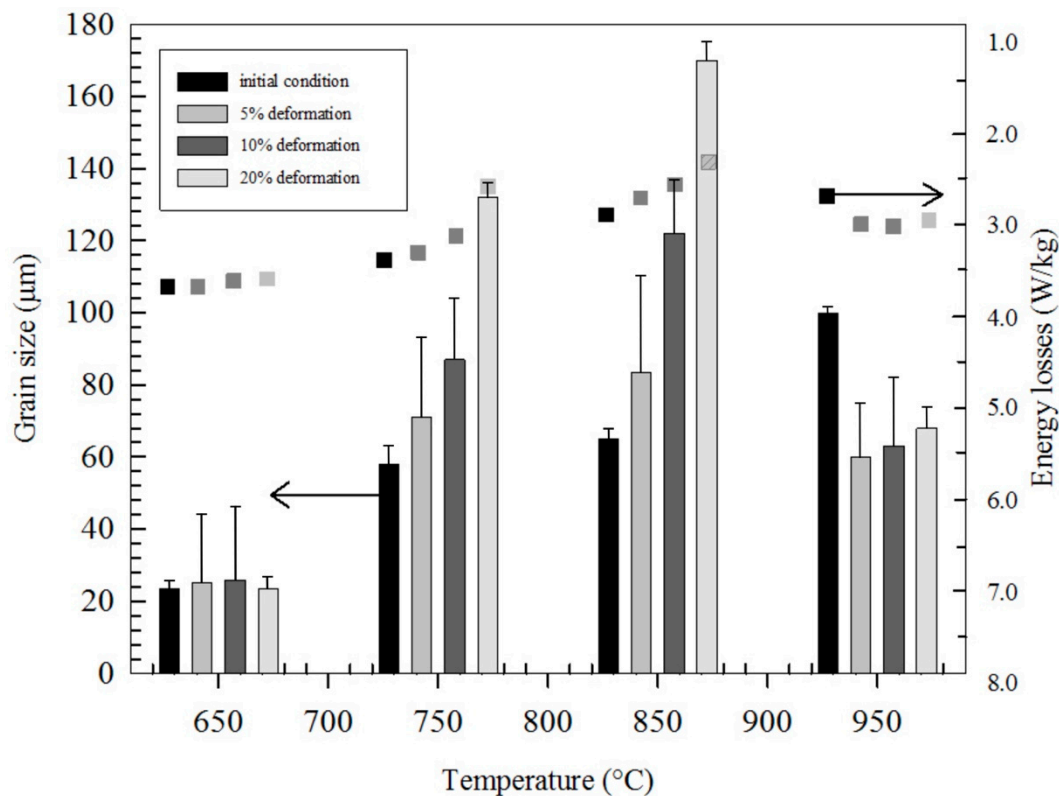


Figure 7. Effect of annealing temperature on grain size-energy losses relationship in deformed electrical steel samples. → energy losses, ← grain size.

4. Conclusions

In this work, the study of the effect of cold deformation on the grain size-magnetic properties relationship, in a commercial electrical steel GNO-type with low Si + Al, was studied, and the following is concluded:

1. Plastic deformation applied to grain non-oriented electrical steel sheets caused a significant increase in energy losses, from 10% for 5% strains to a 50% increase in energy losses for 20% strain, which indicates that the magnetic properties are very sensitive to small deformations. The affection of the properties due to the deformation shows that the dominant mechanism during this process is the interaction of the dislocations with the magnetic domains' walls. However, other microstructural defects as well as residual stresses also play an important role.
2. The microstructural differences observed in this research show that the microstructure can change substantially due to the used processing parameters used, since the microstructural characteristics strongly depend on the deformation imposed on the material prior to the annealing treatment, which can affect or favor the magnetic steel properties.
3. Annealing at different temperatures allows to recovery of the magnetic properties. Experimentally it was shown that small deformations prior to heat treatment provide better results in energy losses. The lowest values were obtained when the steel is annealed in the two-phase range ($\alpha + \gamma$), with a combination of 20% deformation and 850 °C temperature, which produce grain size of 170 μm , allowing energy losses to be reduced in 70%. In contrast annealing in γ -phase produced only limits the recovery in the magnetic losses since growth is limited.
4. The results obtained in this research suggest an attractive processing route to produce electrical steel sheets from a commercial steel grade (% Si + Al < 0.6) with low magnetic hysteresis losses, even lower than those obtained through the conven-

tional route in higher grades of electrical steels, which is beneficial both energetically and economically.

Author Contributions: Conceptualization, N.M.L.-G. and A.S.-R.; investigation, N.M.L.-G. writing—review and editing, E.J.G.-C.; project administration, A.S.-R. and N.M.L.-G.; resources, A.S.-R. and supervision, A.S.-R. All authors have read and agreed to the published version of the manuscript.

Funding: This research received no external funding.

Institutional Review Board Statement: Not applicable.

Informed Consent Statement: Not applicable.

Data Availability Statement: Data sharing is not applicable to this article.

Conflicts of Interest: The authors declare no conflict of interest.

References

1. Honda, A.; Obata, Y.; Okamura, S. History and recent development of non-oriented electrical steel in Kawasaki Steel. *Kawasaki Steel Gihō* **1997**, *29*, 136–141.
2. Hug, E.; Hubert, O.; Clavel, M. Some aspects of the magnetomechanical coupling in the strengthening of nonoriented and grain-oriented 3% Si-Fe alloys. *IEEE Trans. Magn.* **1997**, *33*, 763–771. [[CrossRef](#)]
3. Landgraf, F.J.G.; Teixeira, J.C.; Emura, M.; De Campos, M.F.; Muranaka, C.S. Separating components of the hysteresis loss non-oriented electrical steels. *Mater. Sci. Forum.* **1999**, *302*, 440–445. [[CrossRef](#)]
4. Bacaltchuk, C.M. Effect of magnetic annealing on texture and microstructure development in silicon steel. Doctoral's Thesis, Florida State University, Tallahassee, FL, USA, 2004.
5. Fischer, O.; Schneider, J. Influence of deformation process on the improvement of non-oriented electrical steel. *J. Magn. Magn. Mater.* **2003**, *4*, 302–306. [[CrossRef](#)]
6. Hou, C.K.; Lee, S. Effect of rolling strain on the loss separation and permeability of lamination steels. *IEEE Trans. Magn.* **1994**, *30*, 212–216.
7. Shiozaki, M.; Kurosaki, Y. The effect of grain size on the magnetic properties of nonoriented electrical steel sheets. *J. Mater. Eng.* **1989**, *11*, 37–43. [[CrossRef](#)]
8. Jiles, D.C.; Thoenke, J.B.; Devine, M.K. Numerical determination of hysteresis parameters for the modeling of magnetic properties using the theory of ferromagnetic hysteresis. *IEEE Trans. Magn.* **1992**, *28*, 27–35. [[CrossRef](#)]
9. Bailey, J.E.; Hirsch, P.B. The dislocation distribution, flow stress, and stored energy in cold-worked polycrystalline silver. *Philos. Mag. Lett.* **1960**, *5*, 485–497. [[CrossRef](#)]
10. Otte, H.M.; Hren, J.J. The observation of crystalline imperfections and their role in plastic deformation. *Exp. Mech.* **1966**, *6*, 177–193. [[CrossRef](#)]
11. Kvackaj, T.; Demjan, I.; Bella, P.; Kočiško, R.; Petroušek, P.; Fedorikova, A.; Bidulská, J.; Lupták, M.; Jandačka, P.; Lascákóvá, M. The influence of annealing temperature on the magnetic properties of cry-rolled non-oriented electrical Steel. *Acta Metall. Slovaca* **2022**, *28*, 97–100. [[CrossRef](#)]
12. Degauque, J.; Astie, B.; Porteseil, L.; Vergne, R. Influence of grain size on the magnetic and magnetomechanical properties of high-purity iron. *J. Magn. Magn. Mater.* **1982**, *26*, 261–263. [[CrossRef](#)]
13. Kvackaj, T.; Bidulská, J.; Bidulsky, R.; Kovacova, A.; Kocisko, R.; Bella, P.; Luptak, M.; Bacso, J. Influence of annealing conditions on structural development of cryo rolled FeSi Steel. *Acta Phys. Pol. A* **2014**, *126*, 184–185. [[CrossRef](#)]
14. Chaudhury, A.; Khatirkar, R.; Viswanathan, N.N.; Singal, V.; Ingle, A.; Joshi, S.; Samajdar, I. Low silicon non-grain-oriented electrical steel: Linking magnetic properties with metallurgical factors. *J. Magn. Magn. Mater.* **2007**, *313*, 21–28. [[CrossRef](#)]
15. Landgraf, F.J.G.; Emura, M. Losses and permeability improvement by stress relieving fully processed electrical steels with previous small deformation. *J. Magn. Magn. Mater.* **2002**, *242*, 152–156. [[CrossRef](#)]
16. Li, M.; Xiao, Y.-D.; Wang, W.; Zhou, J.; Wu, G.-L.; Peng, Y.-M. Effect of annealing parameter on microstructure and magnetic properties of cold rolled non-oriented electrical steel. *Trans. Nonferrous Met. Soc. China* **2007**, *17*, 74–78.
17. Park, J.-T.; Szupnar, J.A.; Cha, S.-Y. Effect of heating rate on the development of annealing texture in nonoriented electrical steels. *ISIJ Int.* **2003**, *43*, 1611–1614. [[CrossRef](#)]
18. Lee, K.; Huh, M.Y.; Lee, H.; Park, J.; Kim, J.; Shin, E.; Engler, O. Effect of hot band grain size on development of textures and magnetic properties in 2.0% Si non-oriented electrical steel sheet. *J. Magn. Magn. Mater.* **2015**, *396*, 53–64. [[CrossRef](#)]
19. Pedrosa, J.; Paolinelli, S.; Cota, A. Influence of initial annealing on structure evolution and magnetic properties of 3.4% Si non-oriented steel during final annealing. *J. Magn. Magn. Mater.* **2015**, *393*, 146–150. [[CrossRef](#)]
20. Paolinelli, S.C.; da Cunha, M.A. Development of a new generation of high permeability non-oriented silicon steels. *J. Magn. Magn. Mater.* **2006**, *304*, 596–598. [[CrossRef](#)]
21. Hou, C.K. Effect of hot band annealing temperature on the magnetic properties of low carbon electrical steels. *ISIJ Int.* **1996**, *36*, 563–571. [[CrossRef](#)]

22. ASTM-E112-10; Standard Test Method for Determine Average Grain Size. ASTM International: West Conshohocken, PA, USA, 2010.
23. Foner, S. Vibrating sample magnetometer. *Rev. Sci. Instrum.* **1956**, *27*, 548–558. [[CrossRef](#)]
24. Foner, S. Versatile and sensitive vibrating-sample magnetometer. *Rev. Sci. Instrum.* **1959**, *30*, 548–557. [[CrossRef](#)]
25. ASTM A683-16; Standard Specification for Nonoriented Electrical Steel, Semiprocessed types. ASTM International: West Conshohocken, PA, USA, 2016.
26. Askeland, D.R. *Ciencia e Ingeniería de los Materiales*, 3rd ed.; International Thomson: Mexico City, Mexico, 2000; pp. 37–97.
27. Cullity, B.D. *Elements of X-ray Diffraction, Reading*; Addison-Wesley Publishing Company, Inc.: Boston, MA, USA, 1956; pp. 215–269.
28. Salinas Beltran, J.; Salinas Rodríguez, A.; Gutiérrez Castañeda, E.; Deaquino Lara, R. Effect of processing conditions on the final microstructure and magnetic properties in non-oriented electrical steels. *J. Magn. Magn. Mater.* **2016**, *406*, 159–165. [[CrossRef](#)]
29. Kovac, F.; Stoyka, V.; Petryshynets, I. Strain-induced grain growth in non-oriented electrical steels. *J. Magn. Magn. Mater.* **2008**, *320*, 627–630. [[CrossRef](#)]
30. Gutiérrez Castañeda, E.J.; Salinas Rodríguez, A.; Deaquino Lara, R.; Marquez Torres, F. High temperature oxidation and Its effects on microstructural changes of hot-rolled low carbon non-oriented electrical steels during air annealing. *Oxid. Met.* **2015**, *83*, 237–252. [[CrossRef](#)]
31. Gutiérrez Castañeda, E.J.; Hernández Miranda, M.G.; Salinas Rodríguez, A.; Aguilar Carrillo, J.; Domínguez, R. An EBSD investigation on the columnar grain growth in non-oriented electrical steels assisted by strain induced boundary migration. *Mater. Lett.* **2019**, *252*, 42–46. [[CrossRef](#)]
32. Rodríguez, D.L.; Pascoto, T.S.; Almeida, A.A.; Landgraf, F.J.G.; Martin, R.V. The effect of recovery annealing on the magnetic and mechanical properties of nonoriented electrical steels. *IEEE Trans. Magn.* **2014**, *50*, 1–4. [[CrossRef](#)]
33. Cong, J.Q.; Guo, F.H.; Qiao, J.L.; Qiu, S.T.; Wang, H.J. Texture evolution during recrystallization and grain growth in non-oriented electrical steel plates produced by compact strip production process. *Materials* **2022**, *15*, 197–211. [[CrossRef](#)]
34. Da, C.; Paolinelli, S.C. Effect of annealing temperature on the structure and magnetic properties of 2% Si steel. *Mater. Res.* **2002**, *5*, 373–378.
35. Bertotti, G. Connection between microstructure and magnetic properties of soft magnetic materials. *J. Magn. Magn. Mater.* **2008**, *320*, 2436–2442. [[CrossRef](#)]
36. Landgraf, F.J.G.; Silveira, J.R.F.; Rodríguez, D., Jr. Determining the effect of grain size and maximum induction upon coercive field of electrical steels. *J. Magn. Magn. Mater.* **2011**, *323*, 2335–2339. [[CrossRef](#)]